Dimensionless Analysis of Tire Characteristics for Vehicle Dynamics Studies

Matthew Polley and Andrew G. Alleyne, *Senior Member, IEEE*

Abstract— **This paper demonstrates the use of dimensional analysis for scaled vehicle tires. The motivation for this approach is the understanding of realistic nonlinear tire behavior in scaled vehicle control studies. By examining the behavior of vehicle tires within a dimensionless framework, several key tire parameters are developed that allow for an appropriate relationship between full-sized tires and scaled tires. Introducing these scalings into vehicle dynamics studies allows for the development of scaled vehicles that have a high degree of dynamic similitude with full-sized vehicles but are safer and more economical testbeds on which to develop experimental control strategies. Experimental data is used to compare the nonlinear characteristics for sets of scaled and full-sized tires.**

I. Introduction and Motivation

PREVIOUS work at the University of Illinois [1,2] has laid the groundwork for analyzing the dynamics of vehicles in a dimensionless framework. The basis for this analysis approach is the well known Pi theorem [3] that can be found in many standard textbooks on Fluid Mechanics. Most of the previous dimensionless vehicles studies focused on a typical linear 2 degree of freedom vehicle model known as the "Bicycle Model." The basic form of the model is given in Equation (1).

$$\begin{bmatrix} \dot{V} \\ \dot{r} \end{bmatrix} = \begin{bmatrix} \dfrac{-2(C_{\alpha f}+C_{\alpha r})}{mU} & \dfrac{2(C_{\alpha r}b-C_{\alpha f}a)}{mU}-U \\ \dfrac{2(C_{\alpha r}b-C_{\alpha f}a)}{I_zU} & \dfrac{-2(C_{\alpha f}a^2+C_{\alpha r}b^2)}{I_zU} \end{bmatrix} \begin{bmatrix} V \\ r \end{bmatrix} + \begin{bmatrix} \dfrac{2}{m}C_{\alpha f} \\ \dfrac{2aC_{\alpha f}}{I_z} \end{bmatrix} \delta_f \quad (1)$$

V	Vehicle lateral velocity state
r	Vehicle yaw rate state
m	Vehicle mass
I_z	Vehicle moment of inertia
a	Distance from c.g. to front axle
b	Distance from c.g. to rear axle
$C_{\alpha f}$	Front cornering stiffness
$C_{\alpha r}$	Rear cornering stiffness
δ_f	Steering angle
U	Vehicle longitudinal velocity

A. Alleyne (corresponding author) is with University of Illinois, Urbana-Champaign, 1206 West Green St., Urbana, IL 61801, phone: 217-244-9993, e-mail: alleyne@uiuc.edu.

M. Polley was with the University of Illinois, Urbana-Champaign. He is now with MPC Products in Chicago, IL. (e-mail: polley@illinoisalumni.org)

In [1,2], the equations in (1) were reformulated into a dimensionless framework with several key advantages identified. One advantage is the fact that a dimensionless system representation can elicit underlying parametric relationships that are difficult to uncover in a dimensional formulation. The work presented in [1] determined a duality between the cornering stiffness parameter and the vehicle speed for a typical passenger vehicle. This duality manifested itself as an identical effect on open loop system eigenvalues when examined in a dimensionless setting. Whereas typical dimensioned representations seemed to indicate two separate effects on the vehicle's dynamics, a dimensionless approach illustrated that cornering stiffness and vehicle velocity were, in fact, equivalent in the proper representation. The knowledge of this duality would greatly simplify any gain-scheduling or robust control approach to account for parametric variation if these schemes were formulated in a dimensionless setting.

Other benefits of a dimensionless approach include a drastic reduction in the parametric uncertainty for a standard Bicycle Model representation [4]. The distributions of vehicle dimensionless parameters tend to be tightly clustered about distinct mean values. This relaxes the requirements on robust controllers and gives a much less conservative controller design. A consequence of this can be seen in the uncertainty representations shown in Figures 1 and 2. Figure 1 shows a dimensioned multiplicative uncertainty representation for vehicle dynamics, using a wide sampling of different vehicles, and Figure 2 shows a dimensionless version. The overall uncertainty level is significantly lower in the dimensionless case because parametric coupling has been inherently taken into account.

Additionally, the dimensionless parameters not only cluster about a mean value but they also tend to form distinct functional relationships between themselves [5]. In essence, the dimensionless parameter space is relatively sparsely filled by the different vehicle parameters. For all vehicles produced, the dimensionless form of the parameters tends to lie in a subspace of the overall parameter space. This greatly reduces the burden on any identification algorithm effectively allowing more

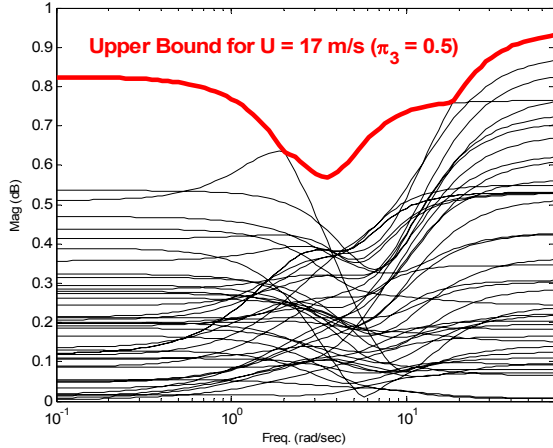information to be gained with less system excitation [5].

Fig. 1: Multiplicative uncertainty bounds for dimensioned form of vehicle dynamics [4].
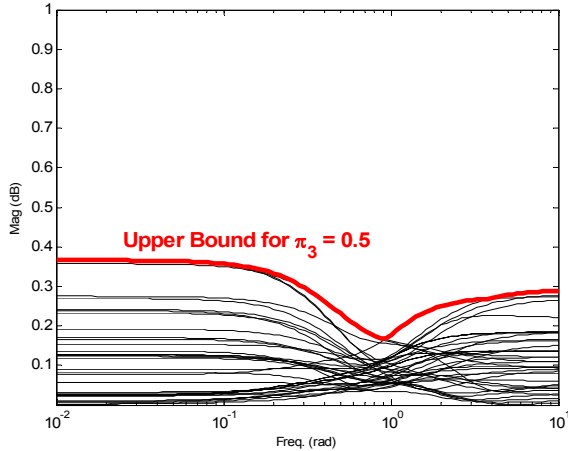

Fig. 2: Multiplicative uncertainty bounds for dimensionless form of vehicle dynamics [4].

All of the previously mentioned work performed for dimensionless representations of the vehicle was done on the linear vehicle model given in Equation (1). This vehicle representation works well for relatively good road surfaces and relatively low lateral accelerations (<0.3 g) of the vehicle [2]. However, it was desired to demonstrate the ability for scaling and dimensional analysis to extend beyond the linear Bicycle Model representation and encompass some of the system nonlinearities. From the point of view of Vehicle Dynamics, the first major nonlinearity encountered is the force-producing characteristics of the vehicle tires. The current work illustrates how certain tire characteristics can be posed in a dimensionless framework and can be shown to exhibit dynamic similitude with full sized tires. Therefore, with proper understanding and system design, scaled vehicles can be utilized for testing of controllers in conditions outside the linear regime.

The rest of this paper is as follows. Section 2 illustrates the experimental hardware system used to generate the data to be analyzed in subsequent sections. Section 3 introduces a particular tire model form, termed the Magic Formula tire model [6] that will be used to analyze the data obtained by the system of Section 2. It will be shown that this model form is *qualitatively* valid for both scaled and full-sized tires as long as both are pneumatic. Section 4 discusses the results of the data and illustrates the dimensionless representation of the tire characteristics that shows *quantitative* similarity between scaled and full-sized tires. Section 5 concludes the paper with a discussion on some of the key points learned as well as their impact for scaled vehicle designs.

II. SCALED TIRE TESTING SYSTEM

Figures 3 and 4 give a front and side view of the experimental apparatus used to generate the scaled tire data in this work. It consists of a frame upon which is mounted a 2 degree of freedom actuation system capable of vertical motion along the z-axis and rotational motion (α) about the z-axis. These two degrees of freedom are controlled by brushless DC motors and used to set the normal force and slip angle of the tire with respect to the road surface. The road surface is a high performance commercial treadmill made by True, Inc. that has its own speed controller integrated and can be controlled between 0 and 5 m/s in 0.1 m/s increments. The tire forces were sensed by a 6-axis force transducer and the tire speed was sensed by an optical encoder that was connected to the wheel axle via a belt and gear. In all tests, the assumption was that the road speed was constant as set by the treadmill controller. All control actions were performed via a DSPACE DS1102 data acquisition system that also recorded the force and velocity data for the tire.

The tire slip angle [7] is the difference between the direction of motion of the tire center and the orientation of the tire longitudinal axis. The tire's longitudinal slip [7] is defined as the difference between the road speed and the tangential speed of the tire's outer surface, which is then normalized by the speed of the road for the braking studies presented here. The tire slip angle is generated by rotating the tire assembly with respect to the direction of treadmill travel. The longitudinal slip is generated by application of a pressure to a small hydraulic brake caliper that is coupled to a steel brake disc attached to the wheel as shown in Figure 4. The braking pressure is controlled by a manually adjusted pressure regulator that was sufficient for the steady state braking tests performed.

Both the z-axis and the slip angle were under closed loop control to maintain accuracy in the data measurements. The z-axis controller was critical to maintain a constant normal force on the tire throughout a particular test. As detailed in [8] a hybrid position/force controller was designed and implemented for the z-axis motion.
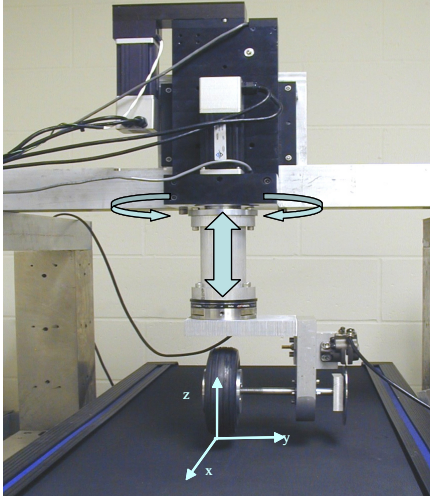
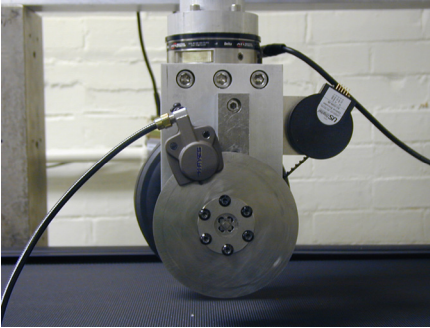**Fig 3: Front view of scaled tire tester showing frame, treadmill, and actuation.**

Fig. 4: Side view of tester showing caliper, brake, force transducer, and encoder.

Fig 5: Four sizes of the scaled tires used for data generation.

The chosen tire type for the testing was the DuBro TV model large scale treaded wheel that was originally designed for model airplanes. This model came in four different sizes ranging in diameter from 4.5 inches (0.114 m) to 6.0 inches (0.152 m), which were all used for the tire testing shown in Section 4. A picture of the four sizes of test tires is shown in Figure 5. This tire type resembles full sized automobile tires in construction, due to a rubber tread design and the fact that the tire is pneumatic, but there are some differences in the tire construction [8]. One difference is the relative shape of the tire. The ratio of the wheel diameter to the outside diameter of the tire is significantly larger for the full sized vehicles. This is attributed to the smaller values of aspect ratio that the full sized tires exhibit (65-70) versus the scaled tires (110). Aspect ratio is

defined as the (100*tire height/tire width). The cross-section shown in Figure 6 gives a better idea of the tread pattern and aspect ratio for the scaled tires. Section 4 further details the impact of varied aspect ratio.
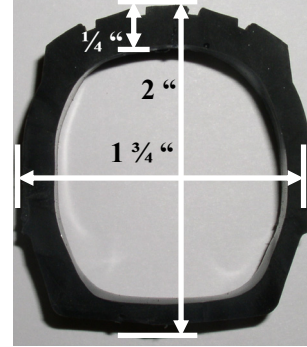

Fig. 6: Cross sectional view of scaled tire used.

III. TIRE MODELING

To define steady state tire response a number of tire models have been developed. Such models have utilized a variety of methods to describe the complex nonlinear phenomenon that a tire exhibits. Models utilizing finite element methods have been developed, as shown in [9], breaking the tire into small 3 dimensional nodes. These models are attractive because they are quite accurate in describing tire response. Although these models can accurately define tire behavior they are computationally intensive and are usually not the best option for real-time vehicle simulations. Other types of models utilize a physical tire model to define tire behavior. An example of such a model is the 'brush' tire model described in [10]. This model defines the tire as a group of elastic/spring-like cylinders positioned radially outside of a circular belt. The resulting model is analytical in nature. The classification of tire models considered for the current research employs the use of empirical models that require testing data for characterization. These models are defined by fitting tire test data to a developed formula. Such functions have been developed using polynomial fits and fits based off of the physical nature of the tire [6].

After examining several types of models, the tire model chosen for the fit of the scaled tire data was the Magic Formula [6]. This model is an empirical model that is widely used due to its ability to accurately define a tire response over its linear and nonlinear regions, without requiring intensive computation. The model parameters include terms that define physical characteristics of the tire. The models for the lateral force, longitudinal force and self aligning moment are summarized as follows.

Lateral Force Model:

$$F_y = D \sin\left[C \tan^{-1}\left(B\Phi_{F_y}\right)\right] + \Delta S_v \qquad (2)$$

$$\Phi_{F_y} = (1-E)(\alpha + \Delta S_h) + \left(E/B\right)\tan^{-1}\left[B(\alpha + \Delta S_h)\right] \qquad (3)$$

$$C = 1.3 \qquad (4)$$

$$C_\alpha = B \cdot C \cdot D \qquad (5)$$

Self Aligning Moment Model:

$$M_z = D\sin\left[C\tan^{-1}\left(B\Phi_{M_z}\right)\right] + \Delta S_v \quad (6)$$

$$\Phi_{M_z} = (1-E)\left(\alpha + \Delta S_h\right) + \left(E/B\right)\tan^{-1}\left[B\left(\alpha + \Delta S_h\right)\right] \quad (7)$$

$$C = 2.4 \quad (8)$$

$$C_{M,\alpha} = B \cdot C \cdot D \quad (9)$$

Longitudinal Force Model:

$$F_x = D\sin\left[C\tan^{-1}\left(B\Phi_{F_x}\right)\right] \quad (10)$$

$$\Phi_{F_x} = (1-E)\lambda + \left(E/B\right)\tan^{-1}\left(B\lambda\right) \quad (11)$$

$$C = 1.65 \quad (12)$$

The lateral cornering stiffness is given in Equation (5) and the slip angle is α and the longitudinal slip is λ. As can be seen in the equations describing the Magic Formula the model utilizes six basic parameters. Two of these parameters, ΔS_v and ΔS_h, are shifts that compensate for intrinsic tire characteristics such as conicity and ply steer. These will not be considered in detail here. The other four terms were all involved in shaping the resulting fit, each having a specific role that is appropriately described by their names [6].

B = Stiffness Factor
C = Shape Factor
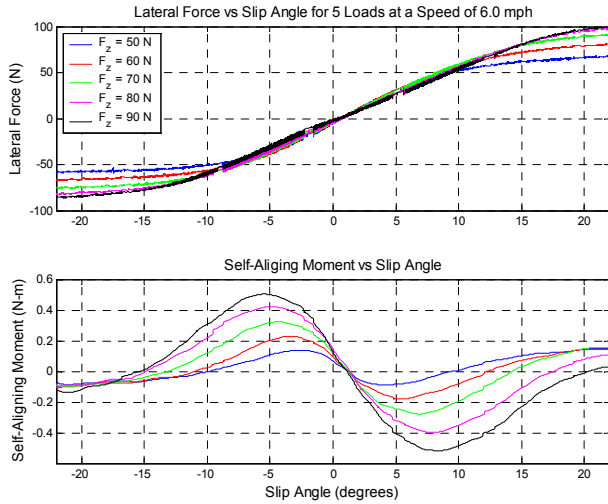D = Peak Factor
E = Curvature Factor

Fig. 7: Lateral force and aligning moment data.

The shape factors used in Equations (4), (8), and (12) are for full sized vehicles [6]. To determine the values of the various parameters for the scaled tires, the experimental system of Section 2 was utilized to determine the lateral force and aligning moment values for different values of slip angle as well as longitudinal force as a function of longitudinal slip. Figure 7 shows the lateral force and aligning moment data for a given tire and loading conditions. Extensive amounts of additional data, including longitudinal force data, can be found in [8] and are not reproduced here due to space limitations. A

comparison with data presented in [6] illustrates a high degree of qualitative similarity between the scaled tire data and full sized tire data.

Diam. (in)	Speed (m/s)	~Load (N)	B	C	D (N)	E	ΔS_v	ΔS_h
4.5	1.3	20	0.132	1.30	21.30	0.04	0.06	-0.59
	1.3	30	0.112	1.23	31.14	-0.62	1.44	-0.67
	1.3	40	0.104	1.15	38.77	-0.99	3.15	-0.90
	1.3	50	0.079	1.18	50.98	-1.71	3.64	-0.99
	1.3	60	0.065	1.35	57.45	-1.05	3.66	-0.92
	1.3	70	0.057	1.43	62.86	-1.17	3.06	-0.82
5.0	1.3	20	0.114	1.67	25.27	1.04	2.48	-0.68
	1.3	30	0.104	1.55	35.99	0.99	2.83	-0.62
	1.3	40	0.081	1.73	44.73	0.90	4.11	-0.76
	1.3	50	0.109	0.96	56.29	-1.22	6.25	-1.08
	1.3	60	0.078	1.25	62.36	-1.10	7.41	-1.32
	1.3	70	0.064	1.22	74.17	-2.24	8.98	-1.54
5.5	1.3	20	0.138	1.68	23.77	1.04	3.41	-0.92
	1.3	30	0.125	1.30	41.91	1.05	5.78	-1.09
	1.3	40	0.110	1.30	51.09	-0.05	6.73	-1.10
	1.3	50	0.119	0.97	59.23	-1.45	8.35	-1.37
	1.3	60	0.096	1.06	69.44	-1.62	9.83	-1.62
	1.3	70	0.075	1.33	78.63	-0.79	10.38	-1.57

Table 1: Scale tire Magic Formula params. (F_y vs. α)

To adapt the resulting data to the Magic Formula tire model, a fit for each tire response was made using a least squares approach. Table 1 gives parameter fits for a lateral force generation test operating at different normal loads. Other fits can be found in [8]. As evidenced in the table, the shape factor C is approximately the same (~1.3) as for full sized vehicles. Other qualitative similarities were determined for the aligning moment and longitudinal force data thereby leading to the conclusion that the force-generating characteristics of scaled pneumatic tires are qualitatively similar to their full-sized counterparts.

IV. SCALED TIRE CHARACTERISTICS

Due to space limitations, the following analysis will focus on a comparison in lateral force generation. Reference [8] gives additional detail on aligning moment comparisons and, to a lesser extent, longitudinal force comparisons. Using the fits described in the previous section, comparisons can be made for various sizes of tires. This can be done using values of cornering stiffness and cornering coefficient. Cornering stiffness is well known to be the slope at the origin of the lateral force versus slip angle curve. Typically, cornering coefficient is defined as a normalization of the cornering stiffness with respect to normal load [7]. This is defined as:

$$CC_\alpha \equiv \frac{C_\alpha}{F_z} \quad (13)$$

Due to the changing value of friction coefficient under the varying tests conditions between scaled and full-sized tires it was decided to use a slightly altered version of the cornering coefficient. To compensate for a possible

difference in tire/road conditions between scaled and full-sized tires a modified cornering coefficient was calculated by dividing the cornering stiffness by the maximum lateral force generated, defined as D in the Magic Formula, thereby giving:

$$CC_{\alpha,D} \equiv \frac{C_\alpha}{D} \qquad (14)$$

This modified value of cornering coefficient was implemented to compensate for the varying value of the coefficient of friction from test to test, depending on the size, normal load and speed of the tire. This technique is similar to those introduced in the non-dimensionalization methods shown in [11], where tire model fits are developed to represent tire response independent of normal load and friction conditions.

Definition	Variable	Dimension
Aspect Ratio	AR	[-]
Tire Diameter	d_t	[L]
Wheel Base	L	[L]
Cornering Coefficient	$CC_{\alpha,D}$	[-1/rad]

Table 2: Variables used for defining tire scaling

The key terms chosen to represent the dimensionless cornering response of the tire are shown in Table 2. Only two of the particular terms have any dimensions: the wheel base of the vehicle, and the diameter of the tire. These two can be transformed into a dimensionless parameter by simply dividing the tire diameter by the length of the wheel base:

$$\Pi_1 = \frac{d_t}{L} \qquad (15)$$

The term in Equation (15) is considered to be the first pi term for the dimensional analysis of a tire. It is essentially the dimensionless size of the tire, relative to the vehicle size. The remaining variables considered are already dimensionless, if radians are considered to not be a dimension. Both of these variables can be considered to be a pi term on their own, but from previous analysis [8] it was noted that there was a relationship between these two variables. The aspect ratio for full sized tires and the scaled tires was significantly different. As a result, the higher aspect ratio scaled tires had proportionately lower cornering coefficients than their full sized counterparts even when tire/road interaction effects were accounted for. The reason why high aspect ratios lead to low cornering coefficients is that the high aspect ratios indicate high sidewalls which, in turn, indicate greater flexibility. The greater flexibility leads to lower load carrying capacity at a given slip angle. To account for this, a second pi term was created that included both the cornering coefficient with respect to the maximum lateral load, $CC_{\alpha,D}$, and the aspect ratio (AR). This second pi term is defined as:

$$\Pi_2 \equiv CC_{\alpha,D} \cdot AR \qquad (16)$$

The effect of the dimensionless representation of cornering coefficient and aspect ratio can be seen in Figures 8 and 9. Figure 8 illustrates the normalized cornering coefficient of Equation (14) for several scaled tires and full sized tires [12]. The entire set of full sized tire data used for Figures 8 and 9 can be found in [8] and is not reproduced here due to space constraints.
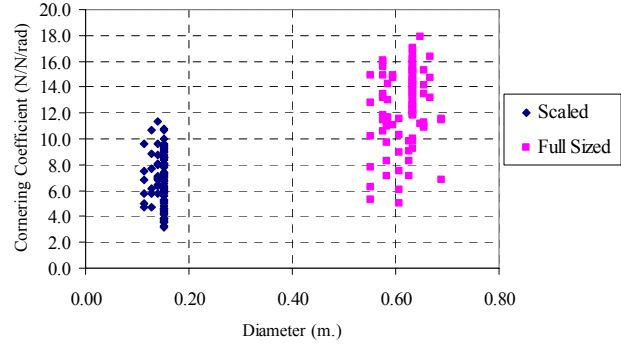

Fig. 8: Cornering coefficients for scaled and full sized [8] tires.

Figure 9 illustrates the Π_2 values for the same distribution of scaled and full sized tires. As evidenced by the results of Figure 9, the distributions of the dimensionless parameter are nearly identical for full sized and scaled tires. Figures 8 and 9 are even more relevant when compared with existing dimensional data shown in Figure 10. Although the values given in Figure 10 are in terms of (1/deg), a conversion from (1/deg) to (1/rad) will indicate that the range of cornering coefficient, and subsequently Π_2, for Figures 8 and 9 exactly matches that of previously established data. The range for of about 4 to 18 $^1/_{rad}$ for $CC_{\alpha D}$ corresponds to 0.1 to 0.3 $^1/_{deg}$ for the cornering coefficient shown in Figure 10. This indicates a *quantitative* match in tire characteristics between scale and full-sized tires to further support the *qualitative* match shown in Section 3.
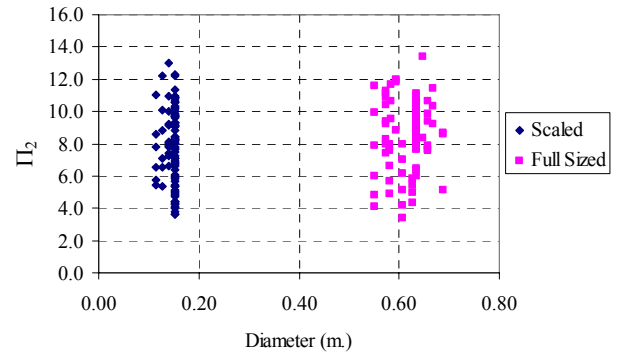

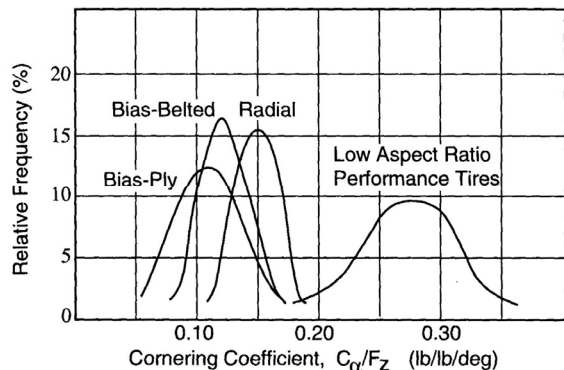**Fig. 9: Π_2 values for scaled and full sized [8] tires**

Fig. 10: Frequency distribution of cornering coefficient values for full sized tires [7].

V. DISCUSSION AND CONCLUSION

The results in Section 3 and 4 demonstrate that the force-producing characteristics of scaled pneumatic tires can exhibit similitude with full-sized tires. The shapes of the force curves are very similar, as shown in Section 3. This was illustrated by nearly identical shape factors between scaled and full sized tires. By appropriate usage of dimensionless descriptions, the nonlinear scale tire characteristics can be made to match those of a full-size tire. The implications for scaled vehicle dynamics and control are as follows. One can use these results to design a scaled vehicle such that it exhibits dynamic similitude for both the linear bicycle model of Equation (1) as well as nonlinear behavior characteristic of low friction or high lateral acceleration maneuvers. As detailed in [8] one could start with a target value of Π_1 and Π_2 for available scaled pneumatic tires and surfaces. From these, one could then determine other key dimensions of the vehicle using the dimensionless analysis and Π parameters developed in [1,2]. This would result in a scaled vehicle designed around the appropriate tire/road interface for dynamic similitude with full sized vehicles.

One interesting insight gained from the analysis of Sections 3 and 4 is as follows. Suppose the lateral force response is crudely simplified into two linear regions that represent the original linear portion and the nonlinear portion of the tire response. This simplification assumes that the tire lateral force linearly approaches its maximum value, with slope C_α, where its response saturates and remains with zero slope for high slip angles. It is known from Equation (14) that the modified cornering coefficient used for this analysis is the ratio of C_α to D and from the discussion of this value it is known that it remains approximately the same for the scaled and full sized automobile tires for tires with similar aspect ratios. Therefore, the slip angle at which the maximum lateral load will occur remains the same for varying tire sizes. Defining α_{max} to be the slip angle of peak lateral force, this invariance with respect to tire size is deduced from the simplified tire response model since:

$$C_\alpha \approx \frac{D}{\alpha_{max}} \qquad (17)$$

$$CC_{\alpha,D} = \frac{C_\alpha}{D} \approx \frac{\left(D/\alpha_{max}\right)}{D} \approx \frac{1}{\alpha_{max}} \qquad (18)$$

This relationship is an approximation from the model simplification, but it shows that the value of the cornering coefficient, $CC_{\alpha,D}$, will be approximately equal to $1/\alpha_{max}$. Since the cornering coefficient remains about the same, so will the value of slip angle at which the maximum load occurs. The value of slip angle (α_{max}) represents the approximate angle at which the tire behavior transitions from a linear to a nonlinear regime. Therefore, the basic response of a tire remains the same as it transitions from partial to full sliding for both full size and scaled tires; even for varying types of tire construction.

REFERENCES

[1] S. Brennan and A. Alleyne, "Robust Scalable Vehicle Control Via Non-dimensional Vehicle Dynamics," *Vehicle System Dynamics*, Vol. 36, Nos. 4-5, Dec. 2001, pp. 255-277.

[2] S. Brennan and A. Alleyne, "Using a Scale Testbed: Controller Design and Evaluation," *IEEE Control Systems Magazine*, Vol. 21, No. 3, 2001, pp. 15-26.

[3] E. Buckingham, "On physically similar systems; illustrations of the use of dimensional equations," *Physical Review,* Vol. 4, No. 4, pp. 345-376, 1914.

[4] S. Brennan and A. Alleyne, "Dimensionless Robust Control With Application To Vehicles," submitted to *IEEE Trans. on Control System Technology*.

[5] S. Brennan and A. Alleyne, "Real-Time Identification of Vehicle Chassis Dynamics Using a Novel Reparameterization Based on Sensitivity Invariance," to appear in the *International Journal of Adaptive Control and Signal Processing*.

[6] E. Bakker, H. B. Pacejka, and L. Lidner, "A New Tire Model with an Application in Vehicle Dynamics Studies", SAE Paper 890087, 1989.

[7] T.D. Gillespie, Fundamentals of Vehicle Dynamics, Warrendale, PA. SAE International, 1992.

[8] M. Polley, "Size Effects On Steady State Pneumatic Tire Behavior: An Experimental Study," M.S. Thesis, M&IE Dept, Univ. of Illinois, Urbana, IL, 2003.

[9] Mastinu, G. and M. Fainello, "Study of the Pneumatic Tyre Behaviour on Dry and Rigid Road by Finite Element Method," *Vehicle System Dynamics*, Vol. 21, pp. 143-165, 1992.

[10] J. Deur, "A Brush-Type Dynamic Tire Friction Model for Non-Uniform Normal Pressure Distribution," 15th IFAC World Congress, Barcelona, 2002.

[11] J. C. Dixon, Tires, Suspension, and Handling, 2nd Edition, Warrendale, PA, SAE International, 1996.

[12] R.W. Allen, R. E. Magdaleno, T. J. Rosenthal, D. H. Klyde, and J. R. Hogue, "Tire Modeling Requirements for Vehicle Dynamics Simulation," SAE Paper 950312, 1995.